Title

Brief Reports: Lysosomal Cross-Correction by Hematopoietic Stem Cell-Derived Macrophages Via Tunneling Nanotubes

Journal

Stem Cells, 33(1)

ISSN

1066-5099

Authors

Naphade, Swati
Sharma, Jay
Chevronnay, Héloïse P Gaide
et al.

Publication Date

2015

DOI

10.1002/stem.1835

Peer reviewed

STEM CELLS®

REGENERATIVE MEDICINE

Brief Reports: Lysosomal Cross-Correction by Hematopoietic Stem Cell-Derived Macrophages Via Tunneling Nanotubes

SWATI NAPHADE,[a] JAY SHARMA,[a] HÉLOISE P. GAIDE CHEVRONNAY,[b] MICHAEL A. SHOOK,[a] BRIAN A. YEAGY,[a] CELINE J. ROCCA,[a] SARAH N. UR,[a] ATHENA J. LAU,[a] PIERRE J. COURTOY,[b] STEPHANIE CHERQUI[a]

Key Words. Hematopoietic stem cells • Macrophages • Tunneling nanotubes • Lysosomal cross-correction • Tubular basement membrane • Cystinosis

[a]Division of Genetics, Department of Pediatrics, University of California, La Jolla, San Diego, California, USA; [b]Cell Biology Unit, de Duve Institute, Université Catholique de Louvain, Brussels, Belgium.

Correspondence: Stephanie Cherqui, Ph.D., Division of Genetics, Department of Pediatrics, University of California, 9500 Gilman Drive, MC 0734, La Jolla, San Diego, California 92093-0734, USA. Telephone: 858-822-1023; Fax: 858-246-1125; e-mail: scherqui@ucsd.edu

Received June 16, 2014; accepted for publication July 23, 2014; first published online in STEM CELLS *EXPRESS* September 3, 2014.

1066-5099/2014/$30.00/0

http://dx.doi.org/10.1002/stem.1835

ABSTRACT

Despite controversies on the potential of hematopoietic stem cells (HSCs) to promote tissue repair, we previously showed that HSC transplantation could correct cystinosis, a multisystemic lysosomal storage disease, caused by a defective lysosomal membrane cystine transporter, cystinosin (*CTNS* gene). Addressing the cellular mechanisms, we here report vesicular cross-correction after HSC differentiation into macrophages. Upon coculture with cystinotic fibroblasts, macrophages produced tunneling nanotubes (TNTs) allowing transfer of cystinosin-bearing lysosomes into Ctns-deficient cells, which exploited the same route to retrogradely transfer cystine-loaded lysosomes to macrophages, providing a bidirectional correction mechanism. TNT formation was enhanced by contact with diseased cells. In vivo, HSCs grafted to cystinotic kidneys also generated nanotubular extensions resembling invadopodia that crossed the dense basement membranes and delivered cystinosin into diseased proximal tubular cells. This is the first report of correction of a genetic lysosomal defect by bidirectional vesicular exchange via TNTs and suggests broader potential for HSC transplantation for other disorders due to defective vesicular proteins. STEM CELLS *2015;33:301–309*

INTRODUCTION

Despite long-standing controversies that hematopoietic stem cells (HSCs) are effective in treating nonhematopoietic diseases, several mechanisms have been proposed to provide tissue repair: cell replacement [1], cell fusion [2], and paracrine/contact interaction [3]. We previously reported that HSCs could correct a nonhematopoietic, multisystemic degenerative disorder, cystinosis, using a validated cystinosis mouse model ($Ctns^{-/-}$) [4, 5]. Cystinosis is a lysosomal storage disorder due to intralysosomal accumulation of cystine in all tissues, leading to early lesions in kidney proximal tubules and eyes, and subsequently evolving into multiorgan failure including end-stage kidney disease, hypothyroidism, myopathy, and neuropathy [6]. The protein defective in cystinosis, cystinosin (*CTNS* gene), is a seven-transmembrane proton-driven cystine transporter bearing two redundant lysosomal targeting signals [4, 7]. In $Ctns^{-/-}$ mice, stable engraftment of bone marrow-derived cells in all organs led to the dramatic reduction in tissue cystine levels in all organs and provided long-term kidney preservation [8–10]. Our recent data pointed to cross-correction, that is, transfer of a functional protein into adjacent deficient cells, as a possible mechanism [8]. However, while cross-correction has been amply demonstrated in several lysosomal storage disorders due to defective soluble lysosomal enzymes by secretion-recapture or enzyme replacement therapy [11], this phenomenon has never been demonstrated for lysosomal transmembrane proteins. In this context, several questions were raised to explain the dramatic impact of HSC transplantation in cystinosis: (a) how do HSCs mediate rescue of nonhematopoietic diseased cells; (b) how can HSCs effectively restore a functional seven-transmembrane transporter in deficient cells; and (c) how can HSC-derived correcting factor(s) penetrate epithelia such as kidney proximal tubular cells (PTCs) that are surrounded by a tight continuous tubular basement membrane (TBM).

Intercellular transport of organelles including lysosomes can occur via tubular extensions mostly known as "tunneling nanotubes" (TNTs), initially reported in vitro [12]

but also recently in vivo [13, 14]. TNTs are heterogeneous cell-connecting tubules that are composed of plasma membrane-bound extensions containing either F-actin alone (thin TNTs, <0.7 μm diameter) or F-actin and microtubules (thick TNTs, >0.7 μm diameter) [15–17]. Often >20 μm in length, TNTs can support long-distance vesicular trafficking in human macrophages [15] and are involved in pathogen spreading and intercellular communication [16, 18]. However, the mechanism of passage across two apposed plasma membranes remains mysterious, and three scenarios have been proposed: (a) transient membrane fusion; (b) organelle release at the nanotube tip and secondary capture by target cells; and (c) engulfment by the recipient cells of bulging nanotube tip with all included organelles ("snapping") [19].

Epithelial basement membranes are specialized cell-associated extracellular matrix (ECM) sheaths that are produced, tightly enclose, and remodeled by epithelial cells [20]. In the kidney, the TBM is a continuous, thick, and dense barrier that strongly limits macromolecules and supramolecular structures to access the tubular cells from the interstitium. The stiffness of TBM is considered comparable to that of articular cartilage [21, 22]. However, ECM can be breached by invadopodia, these highly dynamic, actin-driven membrane protrusions that have the capacity to extend into extracellular matrix and recruit at their tip proteolytic activities such as membrane-type metalloprotease 1, MT1-MMP [23]. Invadopodia have been extensively studied in vitro using cancer cell lines in three-dimensional (3D) matrices and recently described in vivo in *Caenorhabditis elegans* [24–26] but their equivalent in mammalian organisms has still to be defined.

In this study, we demonstrated for the first time that transplanted HSCs led to cross-correction of a lysosomal transmembrane protein after differentiation into macrophages. In coculture with cystinotic fibroblasts, macrophages generated long TNTs acting as intercellular bridges supporting sustained bidirectional lysosomal exchange. In vivo, macrophage-derived tubular extensions resembling invadopodia penetrated the TBM and delivered directly CTNS-containing vesicles into PTCs, suggesting that TNTs and invadopodia are related devices.

Materials and Methods

Mice

C57BL/6 Ctns$^{-/-}$ mice were provided by Dr. Antignac (Inserm U983, Paris, France). DsRed-transgenic mice (B6.Cg-Tg(CAG-DsRed*MST)1Nagy/J) (Jackson Laboratory, Bar Harbor, ME, www.jax.org) were cross-bred with C57BL/6 Ctns$^{-/-}$ mice to produce transgenic DsRed Ctns$^{-/-}$ mice constitutively expressing the DsRed fluorescent protein under the control of the chicken β-actin promoter coupled with the cytomegalovirus immediate early enhancer as previously described [8]. All strains were bred continuously at University of California, San Diego (UCSD) including wild-type C57BL/6 mice and eGFP-transgenic mice (C57BL/6-Tg(ACTB-EGFP)1Osb/J, Jackson Laboratory). All protocols were approved by the AAALAC-Accredited Institutional Animal Care and Use Committee of UCSD.

Cell Culture

Fibroblasts were generated from newborn skin biopsies of C57BL/6 wild-type (WT), Ctns$^{-/-}$, DsRed WT, and DsRed Ctns$^{-/-}$ mice. They were maintained using high glucose DMEM (Dulbecco's modified Eagle's medium; Life Technologies, Carlsbad, CA, www.lifetechnologies.com) supplemented with 10% fetal bovine serum (FBS; Gibco, Life Technologies) and 1% penicillin/streptomycin (PenStrep; Gibco) at 37°C under 5% CO_2.

Mononuclear phagocyte progenitor cells derived from femoral and tibial bone marrow of C57BL/6 WT and eGFP-transgenic mice were propagated in the presence of M-CSF. This macrophage growth factor is secreted by the murine L929 cells [27] and was used as L929 cell-conditioned medium [28]. Flushed bone marrow cells were incubated for 5 minutes in red blood cell lysis buffer. Cells were then passed through a 70-μm cell strainer (BD Biosciences, San Jose, CA, www.bdbiosciences.com) and plated at a density of 10×10^6 in a 10-cm dish in DMEM (Gibco), L929-conditioned media, and 1% penicillin-streptomycin-glutamine (Gibco). After 7–8 days, cells had become firmly adherent to the culture vessel and were fully differentiated. They were characterized by flow cytometry after staining with PECy7-conjugated murine anti-CD45 (BD Pharmingen, BD Biosciences), -CD11b, and -F4/80 antibodies (eBioscience, San Diego, CA, www.ebioscience.com).

The IC-21 macrophage cell line was obtained from American Type Culture Collection (Catalog #TIB-186) and cultured in Roswell Park Memorial Institute (RPMI) 1640 medium (Gibco) supplemented with 10% FBS (Gibco) and 1% PenStrep at 37°C with 5% CO_2 incubation. These trypsin-sensitive cells were harvested into Dulbecco's phosphate buffered saline (PBS; Gibco) using a cell scraper (Fisher Scientific, San Diego, CA, www.fishersci.com). Mesenchymal stem cells derived from the eGFP-transgenic mice (eGFP-MSCs) were generated as described previously [9].

Lentivirus Vector Generation and Production

The SIN-lentivirus vector, pCCL-EFS-X-WPRE (pCCL) was used for gene transfer [29] and contains the intron-less human Elongation Factor 1 alpha promoter (EFS; 242 bp) to drive the transgene expression [30]. The constructs pCCL-eGFP and pCCL-CTNS-eGFP containing the eGFP and the fusion CTNS-eGFP cDNA, respectively, were previously reported [8]. pCCL-Lamp1-DsRed was generated as follows: Lamp1 was amplified from murine cDNA by PCR using the following primers containing the XhoI and BamHI restrictions sites: 5′-ATT CTCGAGATGGCGGCCCCCGGCG-3′ (forward), 5′-GGCGGATCCGA TGGTCTGATAGCCG-3′ (reverse). The PCR product was inserted in phase with DsRed by replacing CTNS in the pCCL-CTNS-DsRed backbone using Xho-I HF and BamHI-HF (New England Biolabs, Ipswich, MA, www.neb.com) restriction sites. Infectious lentiviral particles were produced using the transient tri-transfection procedure in human embryonic kidney 293T cells as previously described [8].

Stable Transduction of Primary Fibroblasts, Primary Macrophages, and IC-21 Cell Line

Six-well plates were coated with Retronectin (20 μl/ml; Takara Bio, Madison, WI, www.takara-bio.com) following the

manufacturer's instructions. Primary Ctns$^{-/-}$ fibroblasts were plated at 2 $\times$ 10^5 cells in 1 ml per well and transduced with either pCCL-CTNS-eGFP or pCCL-Lamp1-DsRed using a multiplicity of infection (MOI) of 20 in presence of 4 μg/ml polybrene (EMD Millipore, Billerica, MA, www.emdmillipore.com). Media were changed 24 hours after transduction. Primary Ctns$^{-/-}$ macrophages were transduced with pCCL-CTNS-eGFP at an MOI of 10 after plating 1 $\times$ 10^5 cells per well. IC-21 macrophages were plated at a density of 3 $\times$ 10^5 cells per well and lentiviral particles of pCCL-eGFP or pCCL-CTNS-eGFP were added at a MOI of 5. Transduction efficiency and stability were verified by flow cytometry.

Transwell and Coculture Assays

For transwell assays, Ctns$^{-/-}$ fibroblasts were plated at 1 $\times$ 10^5 cells per well in six-well plates (BD BioCoat, BD Biosciences). Ctns$^{-/-}$ fibroblasts, eGFP-MSCs, or eGFP-macrophages were plated over transwell inserts at 6 $\times$ 10^4 cells per well. After 14 days of separate coculture at 37°C, transwell inserts were removed and Ctns$^{-/-}$ fibroblasts were harvested using trypsin for cystine measurement.

For contact coculture assays, 4 $\times$ 10^5 DsRed Ctns$^{-/-}$ fibroblasts were plated with 1 $\times$ 10^5 Ctns$^{-/-}$ fibroblasts, eGFP-MSC, pCCL-CTNS-eGFP fibroblasts, or eGFP-macrophages in 10 cm culture dishes. Cells were incubated for 14 days at 37°C, harvested using trypsin, pelleted and resuspended in PBS with 2% FBS, and DsRed fibroblasts were separated using a BD FACS Aria-1 cell sorter prior to processing for cystine content measurement.

Cystine Content Measurement

Cells were resuspended in 150 μl *N*-ethylmaleimide and sonicated for 10 seconds at an amplitude of 2 on ice. Proteins were precipitated using 15% 5-sulfosalicylic acid dihydrate (Fluka Biochemika, Sigma-Aldrich, St. Louis, MO, www.sigmaaldrich.com), resuspended in 0.1 N NaOH, and measured using the Pierce BCA protein assay kit (Pierce, Rockford, IL, www.piercenet.com). Cystine-containing supernatants were sent to the UCSD Biochemical Genetics laboratory for measurement by mass spectrometry as described previously [10].

HSC Isolation, Transduction, and Transplantation

Bone marrow cells were flushed from the long bones of 6–8-week-old eGFP-transgenic mice and DsRed Ctns$^{-/-}$ mice. HSCs were isolated by immunomagnetic separation using anti-Sca1 antibody conjugated to magnetic beads (Miltenyi Biotec, Auburn, CA, www.miltenyibiotec.com). Sca1$^+$ HSCs from eGFP-transgenic mice (eGFP-HSCs) were directly transplanted by tail vein injection of 1 $\times$ 10^6 cells resuspended in 100 μl of PBS into DsRed Ctns$^{-/-}$ mice lethally irradiated (8 Gy) on the previous day. Sca1$^+$ HSCs isolated from DsRed Ctns$^{-/-}$ mice were transduced with pCCL-CTNS-eGFP as previously described [8].

Scanning Electron Microscopy and Transmission Electron Microscopy

Contact cocultures of macrophages and fibroblasts on 12-mm glass coverslips were fixed with 2.5% glutaraldehyde in 0.1 M cacodylate buffer (pH 7.3), buffer-washed, and postfixed in buffered 1% osmium tetroxide. For scanning electron microscopy (SEM), samples were extensively washed in buffer followed by distilled water, dehydrated in graded ethanol series, processed through a critical point dryer (Tousimis Autosamdri 815), and mounted onto SEM stubs with carbon tape. After sputter coating with iridium at 10 μA (EMS model 150T S), preparations were viewed with a Hitachi S-4800 SEM (Hitachi, Pleasanton, CA, www.hitachi.us).

For transmission electron microscopy (TEM), glutaraldehyde- and osmium-fixed samples were buffer washed, treated "en bloc" with 0.5% tannic acid and 1% sodium sulfate, buffer washed, dehydrated in ethanol series, transitioned in 2-hydroxypropyl methacrylate, and embedded in LX112 (Ladd Research, Williston, VT, www.laddresearch.com). Pieces of the flat embedded resin containing cells were glued to a blank block face and 60-nm ultrathin sections were cut, mounted on copper slot grids coated with parlodion, and stained with uranyl acetate and lead citrate. Grids were examined in a Philips CM100 electron microscope (Field Emission Inc.) operating at 80 kV and images were collected using a Megaview III CCD camera (Olympus Soft Imaging Solutions GmbH).

Live Confocal Microscopy and Image Analysis

CTNS-eGFP- or eGFP-macrophages (75,000) were cocultured with equal number of DsRed WT, DsRed Ctns$^{-/-}$, or Lamp1-DsRed Ctns$^{-/-}$ fibroblasts in MatTek glass-bottomed culture dishes (MatTek Corp., Ashland, MA, www.mattek.com).

Confocal imaging was performed on days 3 and 4 using Perkin Elmer UltraView Vox Spinning Disk Confocal (Neuroscience department, Light Microscopy Facility, UCSD School of Medicine) with $\times$40 (Numerical Aperture (NA) = 1.30) and $\times$60 (NA = 1.42) oil objective at 37°C under 5% CO_2. For TNT quantification, images of 60 fields representative of the entire coculture assay dish were captured, processed, and analyzed using Volocity software (Perkin Elmer, Waltham, MA). TNTs formed between eGFP- and CTNS-eGFP-expressing IC21 macrophages and DsRed Fibroblasts (WT and Ctns$^{-/-}$) were manually counted using the "Tools-measure" feature of the software. The tracking of CTNS-eGFP-containing vesicles inside TNTs was performed using the "Track objects manually" feature in Volocity software. The velocities of vesicles moving in one continuous motion without stopping or slowing down were determined.

Immunofluorescence Analysis

Cocultures of CTNS-eGFP macrophages and DsRed Ctns$^{-/-}$ fibroblasts were stained with 100 nM LysoTracker-Blue DND-22 (Life Technologies) added to prewarmed complete phenol red-free RPMI. Following incubation for 3 minutes at 37°C, the medium was replaced with fresh medium. CTNS-eGFP macrophages (50,000) were plated with equal number of Ctns$^{-/-}$ fibroblasts on collagen-coated 0.17 mm coverslips (Fisher Scientific). On day 3, these cocultures were stained with AlexaFluor647-phalloidin (1:100 for 30 minutes; Molecular Probes, Eugene, OR) and rat anti-mouse tubulin (1:600; Abcam, Cambridge, MA, www.abcam.com) followed by Cy5-conjugated goat anti-rat antibody (1:200; Life Technologies). Furthermore, cells were stained with 4′,6-diamidino-2-phenylindole,dihydrochloride (DAPI) (1:500 for 5 minutes; Life Technologies), and coverslips were mounted with ProLong Gold antifade reagent (Life Technologies).

Tissues were fixed in 5% formaldehyde, equilibrated in 20% sucrose overnight, and frozen in Tissue-Tek Optimal Cutting Temperature buffer at −80°C (Sakura Finetek, Torrance,

CA, www.sakura-americas.com). Sections (10-μm) were cut on the Leica CM1860 cryostat and stained with DAPI and AlexaFluor647-phalloidin (1:100 for 30 minutes; Life Technologies). Tissues were also labeled with rat anti-mouse F4/80 antibody (1:25; eBioscience), goat anti-mouse megalin antibodies (1:200; P20 Santa Cruz Biotechnology, Dallas, TX, www.scbt.com) followed by Cy5-conjugated goat anti-rat antibody (1:200; Life Technologies), and DyLight 649 donkey anti-goat (1:200; Jackson ImmunoResearch, West Grove, PA, www.jacksonimmuno.com), respectively. Sections were stained with DAPI and coverslips were mounted using ProLong Gold antifade reagent as above.

Images were acquired using a ×63 (NA = 1.30) glycerol objective on Leica TCS SP5 II confocal microscope. All images were 8-bit optical image slices (series at 0.8-μm interval) acquired using LASAF software (Leica Microsystems, Buffalo Grove, IL, www.leica-microsystems.com) and processed with the Volocity software (Perkin Elmer, Waltham, MA, www.perkinelmer.com) to generate 3D reconstruction series of optical slices (Z-stacks).

To visualize TNTs across basement membrane, kidneys were perfusion-fixed through the left ventricle with 4% formaldehyde, equilibrated overnight in 20% sucrose, and embedded in Tissue-Tek Optimal Cutting Medium (Sakura Finetek). Thick frozen sections (5 μm) were permeabilized with PBS/0.3% Triton X-100 for 5 minutes, incubated for 1 hour with 10% bovine serum albumin (BSA) (Fisher Scientific) and 3% milk to block nonspecific sites, then incubated overnight at 4°C with a combination of biotinylated Lotus Tetragonolobus (LT)-lectin (1:200; B-1325; Vector Labs, Burlingame, CA, www.vectorlabs.com), goat anti-GFP (1:250; ab-6673; Abcam), and rabbit anti-laminin (1:100; L9393; Sigma-Aldrich) in blocking buffer. After washing, sections were incubated with a combination of AlexaFluor 647 donkey anti-rabbit, AlexaFluor488 donkey anti-goat, and AlexaFluor 405 streptavidin (all from Life Technologies) for 1 hour at room temperature in 10% BSA/0.3% Triton X-100 (Promega, Madison, WI, www.promega.com), then mounted with Dako Faramount Aqueous Mounting Medium (Dako, Carpinteria, CA, www.dako.com). Z-stack images were acquired on a spinning disk confocal microscope using a Plan-Apochromat ×100 (NA = 1.4) Oil DIC objective (Cell Observer Spinning Disk; Zeiss, Oberkochen, Germany, www.zeiss.com) and merged with AxioVision Rel 4.8.2.

Statistical Analyses

Significance of differences in TNT numbers and length was analyzed using Student's paired *t* test. One-way ANOVA was used to study significance of differences in cystine contents in transwell and contact coculture assays. All analyses were performed using PRISM 6 software (GraphPad Cary, NC, www.graphpad.com). $p < .05$ was considered as statistically significant.

Results and Discussion

HSCs Differentiate into Macrophages After Transplantation

To elucidate the mechanism of HSC-mediated tissue repair, we developed a novel mouse model, in which Ctns$^{-/-}$ mice back-crossed on a DsRed background so as to ubiquitously express the DsRed reporter gene [8] were transplanted at 2 months of age with eGFP-expressing HSCs derived from eGFP-transgenic mice and analyzed 6 months later. This bifluorescent mouse model not only allows us to track the fate of transplanted HSCs in an in vivo setting but also enables sensitive identification and unequivocal discrimination of events such as fusion, differentiation, and transdifferentiation. In this model, we demonstrated that most of the eGFP^{+} HSC-derived cells in the liver and kidney did not express DsRed (Supporting Information Fig. S1B, S1E), thereby excluding cell fusion as the main mechanism for tissue repair. In these tissues, most eGFP^{+} bone marrow-derived cells also expressed the macrophage marker F4/80 (Supporting Information Fig. S1C, S1F), consistent with our previous suggestion that HSC-derived cells differentiate into tissue-resident macrophages [8–10]. These data also excluded transdifferentiation of HSCs into tissue-specific cell types as mechanism for tissue repair in cystinosis and implied instead a paracrine mode of action.

Direct Cell:Cell Contact is Necessary for Cross-Correction in Cystinosis

To investigate in vitro the local communication events underlying cell-based therapy in cystinosis, we further used our mouse models as source of wild-type (WT) eGFP-macrophages, eGFP-mesenchymal stem cells (MSCs), and Ctns$^{-/-}$ DsRed fibroblasts for coculture experiments. Two mechanisms could account for the transfer of a transmembrane protein from donor to host cells: indirectly by shedding of microvesicles/exosomes [31], or by direct cell:cell contact. Other groups have reported that microvesicles shed by MSCs or by transduced insect cells containing cystinosin and/or its mRNA could lead to substantial decrease in cystinotic fibroblast cystine levels [32, 33]. We found that when eGFP-MSCs and eGFP-macrophages were cocultured with DsRed-Ctns$^{-/-}$ fibroblasts, cystine levels decreased by ∼75% in fluorescence-activated cell-sorted (FACS) fibroblasts (Fig. 1A). In contrast, when the two populations were physically separated using a transwell porous to microvesicles/exosomes [34], cystine levels decreased only by ∼20% (Fig. 1B). These findings suggested that direct cell:cell contact is the main pathway for cross-correction.

Using confocal (Fig. 1C) and scanning electron microscopy (SEM) (Fig. 1D) of eGFP-macrophages and DsRed Ctns$^{-/-}$ fibroblasts cocultures, we found that macrophages extended long TNTs (∼40 μm in average length) that established contact with the fibroblasts, which were strong enough to resist critical-point drying used for SEM (Fig. 1D). Thus, TNTs were potential candidates for mediating cross-correction for cystinosin.

TNTs Mediate Cross-Correction by Transfer of cystinosin-Bearing Lysosomes

To determine whether TNTs could mediate the physical transfer of cystinosin-bearing vesicles from WT macrophages to cystinotic fibroblasts, we cocultured DsRed-Ctns$^{-/-}$ fibroblasts with a macrophage-like IC21-cell line, stably transduced to express cystinosin-eGFP fusion protein (CTNS-eGFP-IC21 macrophages). Time-lapse confocal microscopy revealed that vesicles containing cystinosin-eGFP could migrate along TNTs toward DsRed-Ctns$^{-/-}$ fibroblasts (Fig. 1F and Supporting Information Video S1A). LysoTracker staining identified these

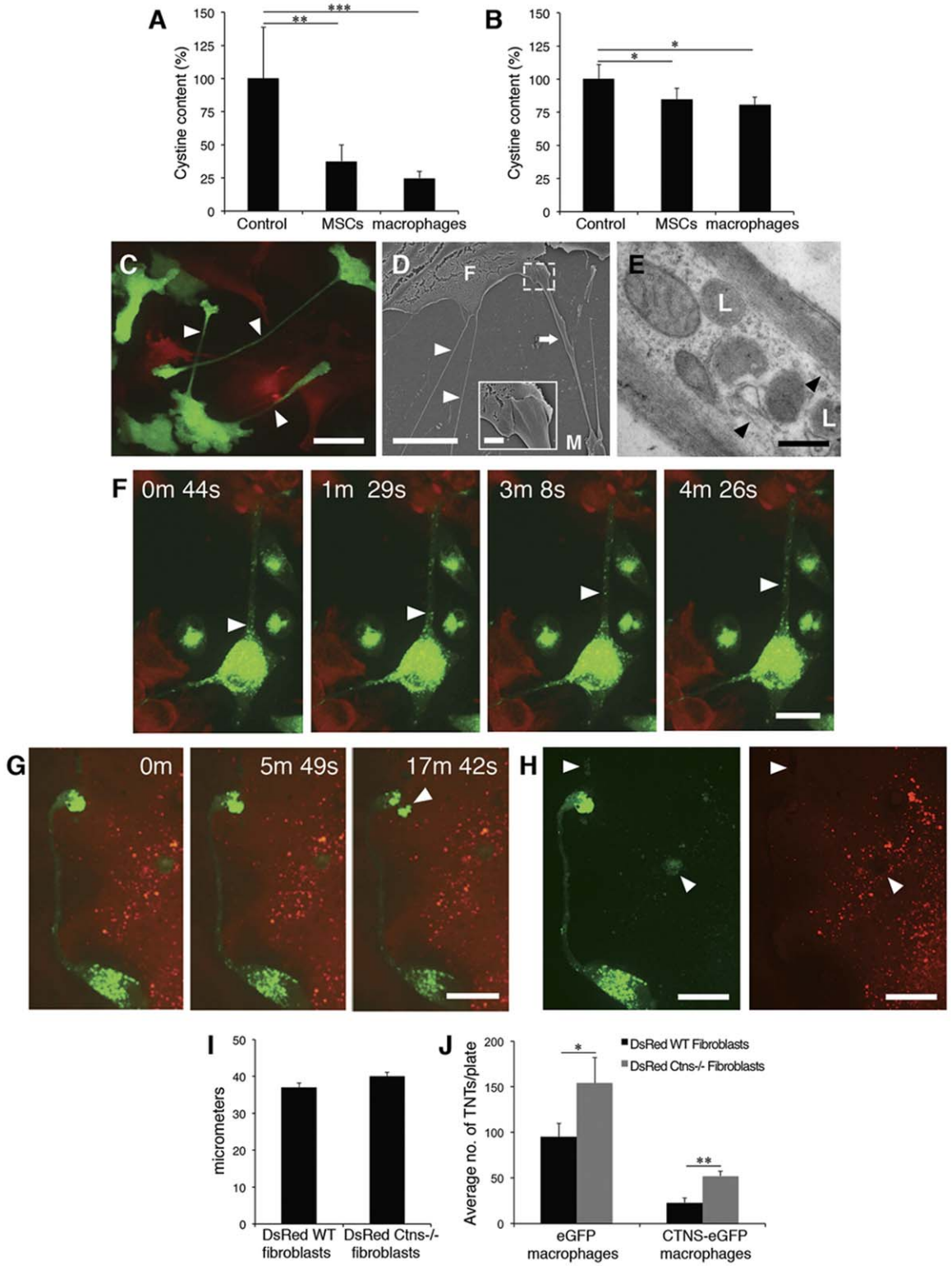

Figure 1. TNT-mediated transfer of cystinosin is the preferred mode of cross-correction. **(A, B):** Histograms representing percent decrease in cystine content in DsRed-Ctns$^{-/-}$ fibroblasts (recipient cells) when plated together with (A: contact coculture assays) or separated by 1-μm pore transwell filters from (B: transwell assays) either eGFP-MSCs or eGFP-macrophages (donor cells) ($n = 4$ replicates for each). Values are means ± SD. *, $p < .05$; **, $p < .01$; ***, $p < .005$. **(C):** Confocal image of TNTs (arrowheads) extended from eGFP-macrophages to DsRed-Ctns$^{-/-}$ fibroblasts. **(D):** Scanning electron micrograph showing two thin TNTs (arrowheads) and one thick (arrow) TNT bridging a primary macrophage (M) and a Ctns$^{-/-}$ fibroblast (F). The connection (box) is enlarged in the inset. **(E):** Transmission electron micrograph showing a thick TNT containing various organelles, including lysosomes (L), along microtubules (arrowheads). **(F):** Representative frames from a confocal imaging movie (Supporting Information Video S1A) showing migration of cystinosin-eGFP-containing vesicles via TNTs from a CTNS-eGFP-expressing macrophage toward DsRed-Ctns$^{-/-}$ fibroblasts (arrowheads). **(G):** Representative frames from a confocal imaging movie (Supporting Information Video S2A) showing bulk fission of a dilated tip of a TNT, delivering a pool of cystinosin-eGFP-containing vesicles to a DsRed-Ctns$^{-/-}$ fibroblast (arrowhead). **(H):** Individual vesicles (arrows) were observed in the cytoplasm of the recipient fibroblasts, probably originating from further dissociation of the internalized pools (arrowheads; Supporting Information Video S2B). **(I, J):** Ctns$^{-/-}$ cells enhance TNT formation, not elongation. Length of TNTs derived from eGFP-IC21 macrophages (I), and average number of TNTs extended by eGFP-IC21 and CTNS-eGFP-IC21 (J) macrophages, estimated after 3 days of coculture with either DsRed-WT or -Ctns$^{-/-}$ fibroblasts ($n = 4$ replicates). Values are means ± SEM. *, $p < .05$; **, $p < .01$. Bars = (C) 30 μm; (D) 10 μm; (D, inset) 1 μm; (E) 500 nm; (F–H) 20 μm. Abbreviations: CTNS, cystinosin; MSC, mesenchymal stem cell; TNT, tunneling nanotube; WT, wild type.

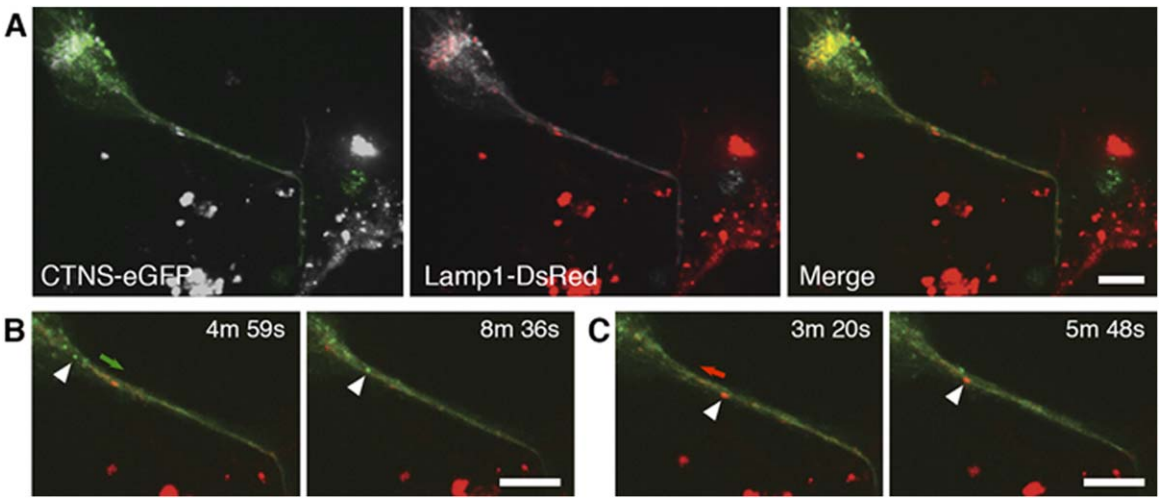

Figure 2. Lysosomal trafficking within tunneling nanotubes (TNTs) is bidirectional. **(A):** Representative frame from a confocal imaging movie (Supporting Information Video S3) of Lamp1-DsRed-expresssing Ctns$^{-/-}$ fibroblasts cocultured with CTNS-eGFP-expressing macrophages showing eGFP- and DsRed-positive lysosomes trafficking via the same TNT. **(B):** The green arrow marks the trajectory toward the Ctns$^{-/-}$ fibroblast of a selected cystinosin-eGFP-containing lysosome (arrowhead) at the two indicated time intervals. **(C):** The red arrow marks the trajectory toward the macrophage of a selected Lamp1-DsRed-containing lysosome (arrowhead) at the two indicated time intervals. Consistent with previous studies [38], abnormally large lysosomes were observed in Ctns$^{-/-}$ fibroblasts. Bar = 10 μm. Abbreviation: CTNS, cystinosin.

vesicles as late endosomes/lysosomes (Supporting Information Fig. S2A). Similar data were obtained with primary macrophages derived from Ctns$^{-/-}$ mice stably expressing cystinosin-eGFP (Supporting Information Video S1B).

Cystinosin-containing vesicles often stalled or reversed direction before moving forward again. Overall, cystinosin-containing vesicles migrated at an average speed of 1 μm/second (ranging from 0.45 to 1.67 μm/second; $n = 24$ tracked vesicles). These features are classic attributes of microtubule-based saltatory motion [15]. By immunofluorescence, thick TNTs containing cystinosin-bearing vesicles were labeled with tubulin (Supporting Information Fig. S2B). By TEM, sections of thick TNTs showed a dense microfilamentous sheath surrounding a central channel with various organelles including lysosomes and mitochondria and with visible microtubules (Fig. 1E).

A major question remained: how are lysosomes bearing correcting functional cystinosin passed from one cytoplasm to the other? In our coculture system, we observed TNT tips to bulge, appose, and apparently merge with their target cell (Fig. 1C, 1D). Furthermore, time-lapse imaging disclosed free vesicle passage between donor and recipient cytoplasm (Supporting Information Video S3). We also observed the tips of the tubular extensions to snap, thereby delivering a pool of cystinosin-containing lysosomes to the deficient cells (Fig. 1G and Supporting Information Video S2A), a possibility previously suggested by Wang and Gerdes [19]. Many individual CTNS-containing lysosomes were present in the cytoplasm of the fibroblast (Fig. 1H), probably released by further fission of the internalized pools (Supporting Information Video S2B). To the best of our knowledge, these data are the first evidence of TNT snapping supporting a cross-correction mechanism.

When Ctns$^{-/-}$ fibroblasts were replaced by DsRed-WT fibroblasts, the length of TNTs from eGFP-IC21 macrophages remained the same (Fig. 1I); however, fewer TNTs were observed (Fig. 1J; ~30% decrease, $p < .05$). A more pronounced difference was observed when TNTs containing cystinosin-bearing vesicles were exclusively quantified using CTNS-eGFP-IC21 macrophages (Fig. 1J; ~55% lower, $p = .001$). These data showed that Ctns-deficient cells triggered nanotube formation, especially the thick TNTs involved in cystinosin transfer. These data are consistent with previous reports indicating that "cellular stress" significantly enhanced TNT formation and organelle transfer [35, 36]. As macrophages and fibroblasts are plated for coculture at a low density so that cells are not in physical contact, the hypothesis is that *Ctns*$^{-/-}$ fibroblasts, because of their defects, secrete in the culture media factors stimulating the generation of TNTs.

TNT-Mediated Lysosomal Transfer is Bidirectional

Having found that cystinosin-bearing lysosomes can use TNTs to reach the cytoplasm of Ctns-deficient cells, we conversely investigated whether defective (cystine-loaded) lysosomes from deficient fibroblasts could also use TNTs to enter the cytoplasm of macrophages. Our bifluorescent assay revealed numerous DsRed-positive vesicles within the eGFP-macrophages (Supporting Information Fig. S2C), suggesting that vesicular transfer via TNTs may indeed be bidirectional. To test this hypothesis, Ctns$^{-/-}$ fibroblasts stably expressing a Lamp1 (Lysosomal-associated membrane protein 1)-DsRed fusion protein were cocultured with CTNS-eGFP-macrophages. Time-lapse confocal imaging confirmed bidirectional transfer of cystinosin- and Lamp1-vesicles along the same TNT (Fig. 2A and Supporting Information Video S3), that is, not only cystinosin-eGFP-containing vesicles migrating toward Ctns-deficient cells (Fig. 2B) but also cystinosin-deficient Lamp1-DsRed lysosomes/endosomes being transferred to the macrophages (Fig. 2C). Lysosomes are dynamic organelles that distribute load by fusion/fission [37]. We thus suggest that active bidirectional lysosomal exchange followed by fusion with the large

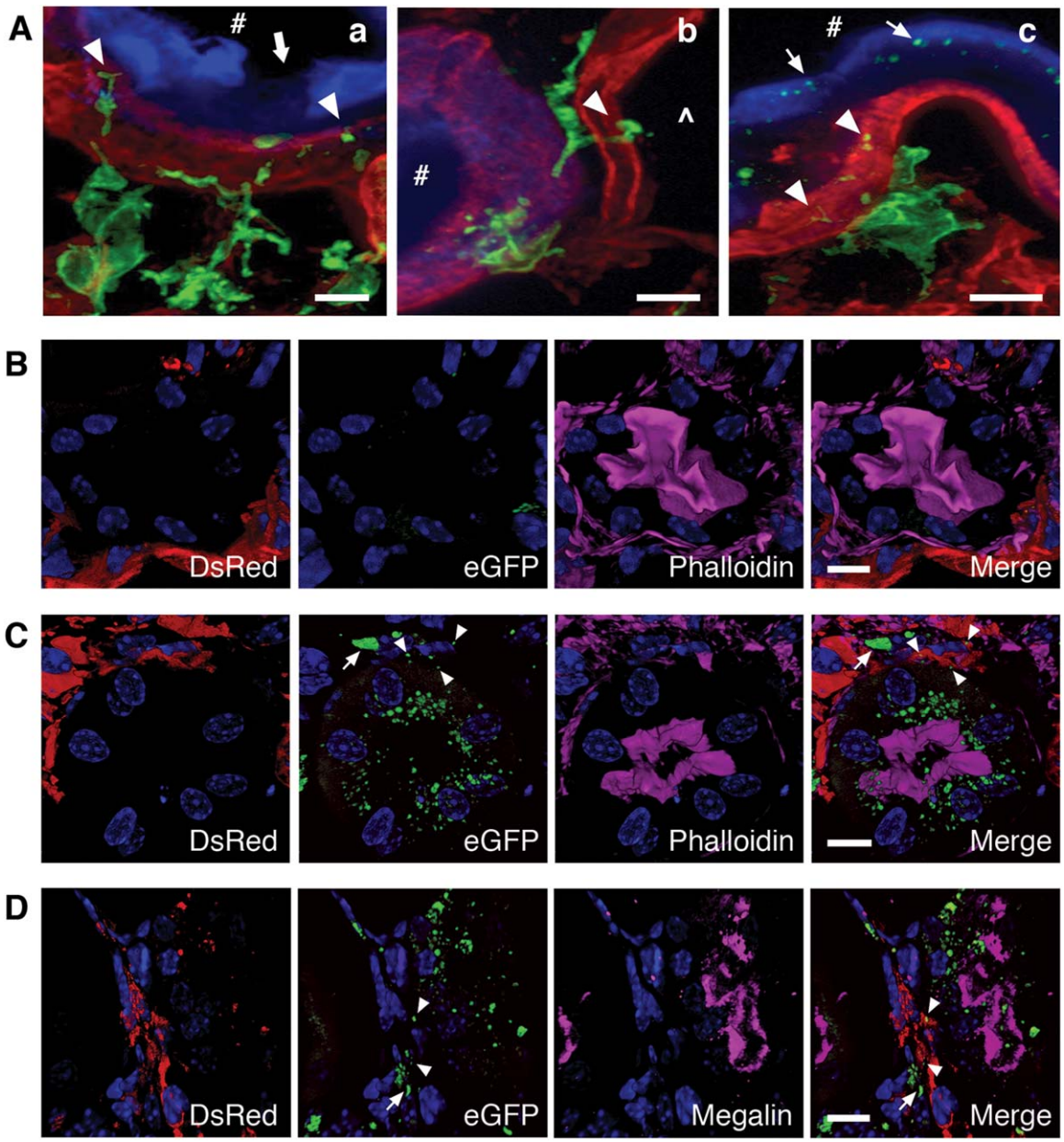

Figure 3. Tunneling nanotube-mediated cystinosin transfer in vivo, study of the kidney. **(A):** Z-stack projections over 7 μm of confocal optical sections from an 8-month-old $Ctns^{-/-}$ mouse kidney, transplanted at 2 months with eGFP-expressing wild-type hematopoietic stem cell (HSC). Green, immunolabeled eGFP; red, laminin immunolabeling provides a grazing view of basement lamina; blue, proximal tubular cell (PTC) brush border-specific sugars labeling by Lotus Tetragonolobus (LT)-lectin defines PTCs (lumen, #). (a) eGFP-expressing HSC-derived cells display numerous tortuous extensions, which frequently appose onto the tubular basement membrane (TBM) of PTCs and show enlarged tips. Arrowheads indicate TBM crossing. Arrow indicates local lack of LT labeling of the PTC epithelium due to dedifferentiation or shedding (for three-dimensional rotation, see Supporting Information Video S4A). (b) At left, multiple extensions entering TBM of a PTC; mottled aspect of BM can be seen. At right, extension crossing TBM of another tubular section not labeled by LT (^). (c) Transferred material appearing as eGFP-expressing green structures become clustered in PTC apical cytoplasm (arrows) (Supporting Information Video S4B). **(B–D):** Z-stack projections of kidneys obtained from $Ctns^{-/-}$ mice transplanted with DsRed-$Ctns^{-/-}$ HSCs (control, B) or DsRed-$Ctns^{-/-}$ HSCs lentivirally transduced to express cystinosin-eGFP (C, D), after labeling for F-actin (phalloidin, magenta, C) or megalin immunolabeling to identify the brush border of proximal tubules (magenta, D). Engrafted DsRed-expressing bone marrow-derived macrophages surrounding kidney tubules contain eGFP-positive discrete vesicles (arrowheads; C and D) or enlarged structures (arrow; C), probably due to clustering and/or fusion of lysosomes due to *CTNS* over-expression, as previously described [8, 38]. Note the abundance of discrete cystinosin-eGFP-containing vesicles in the cytoplasm of transduced PTCs (C, D). Since not all DsRed-HSCs were transduced, some do not express CTNS-eGFP. Nuclei are stained in blue (DAPI). Bars = (A) 5 μm; (B–D) 10 μm.

lysosome pool of cell bodies in the two populations enhances cystine clearance, which probably contributes to the robust decrease in cystine levels observed in all tissues of HSC-transplanted cystinotic mice (57%–94% clearance), despite the limited integration of bone marrow-derived cells within tissues (5%–19%) [9].

In Vivo Cystinosin Transfer from HSC-Mediated Macrophages

Very little is known about TNTs in vivo. We thus examined whether intercellular vesicular exchange involving nanotubules or similar cellular extensions could be detected in vivo, so as to account for the efficacy of HSC grafting in Ctns$^{-/-}$ mice. As proof-of-concept, we focused on the kidney since (a) it represents a particularly challenging tissue for stem cell therapy, because of the formidable TBM barrier enclosing targeted PTCs [21, 22]; (b) the earliest occurrence of cystinosis in PTCs is a major clinical concern; and (c) the mechanism of HSC-mediated renal repair is much debated [39, 40]. Conventional confocal microscopy analysis of kidneys of bifluorescent grafted mice at 6 months post-transplantation revealed abundant bone marrow-derived cells closely surrounding, but never within, the proximal tubules (Supporting Information Fig. S1E, S1F). However, careful high-resolution examination of fields with grazing BM sections revealed numerous tubular extensions emanating from engrafted eGFP-expressing HSC-derived macrophages that penetrated and even crossed the TBM (Fig. 3Aa–3Ac and Supporting Information Videos S4A, S4B). Several tubular extensions could be generated by each macrophage, connecting with several *Ctns*$^{-/-}$ tubular cells, probably accounting for the robust cystine decrease despite limited bone marrow-derived cells present in the tissues [9]. Enlarged tips were reminiscent of those seen in vitro (Fig. 1C) and appeared overall quite comparable to invadopodia [23, 24]. We speculate that epithelial stress in Ctns$^{-/-}$ PTCs (Fig. 3Aa and [41]) promotes TNT/invadopodia formation. As a nonmutually exclusive mechanism, disorganized TBM due to epithelial disease might favor TNTs/invadopodia permeation.

Furthermore, eGFP-containing structures were observed within PTCs, indicating physical transfer of cytoplasm from the macrophages into the epithelia (Fig. 3Ac). To test this hypothesis, we analyzed Ctns$^{-/-}$ mice transplanted with DsRed-Ctns$^{-/-}$ HSCs stably expressing cystinosin-eGFP fusion protein (Fig. 3C, 3D) or with control DsRed-Ctns$^{-/-}$ HSCs (Fig. 3B). Numerous cystinosin-eGFP-containing vesicles were observed in PTCs (Fig. 3C, 3D), directly demonstrating epithelial cell cross-correction and likely accounting for the long-term kidney preservation in Ctns$^{-/-}$ mice [10]. To our knowledge, this is the first evidence of direct transfer of proteins from interstitial macrophages to epithelial cells via TNTs/invadopodia penetrating the TBM, so as to correct a genetic defect leading to PTC degeneration.

Conclusions

We describe here a new mechanism by which HSCs can lead to tissue repair in the context of a lysosomal storage disorder. These findings show that HSC transplantation holds not only potential to treat hematopoietic diseases but also nonhematopoietic disorders, even complex nephropathies. Sustained intercellular, bidirectional vesicular transfer after HSC transplantation, even across the formidable barrier of basement membranes, brings new perspectives to regenerative medicine. In principle, this strategy should be applicable to other lysosomal and even other organelle disorders in which curative therapy requires restoration of the functional protein in multiple tissue compartments, and for which HSC transplantation is yet to be considered.

Acknowledgments

We gratefully acknowledge Corinne Antignac (Inserm U983, Paris, France) for providing the original Ctns$^{-/-}$ mice. This work was funded by the Cystinosis Research Foundation (both laboratories) and NIH Grants RO1-DK090058, R21-DK090548, and RO1-DK099338 (to S.C.). J.S. and M.A.S. were funded by California Institute of Regenerative Medicine, awards TB1-01177 and TB1–01186, respectively. All microcopy work at UCSD was funded by UCSD Neuroscience Microscopy Shared Facility Grant P30 NS047101. Microscopy at Brussels was supported by Belgian F.R.S., at which HGC is Postdoctoral Researcher, National Lottery, Région Bruxelloise, Région Wallonne, UCL, and de Duve Institute sponsorship. We thank Malcolm Wood for his help with electron microscopy.

Author Contributions

S.N.: collection and/or assembly of data, data analysis and interpretation, and manuscript writing; J.S., H.P.G.C., M.A.S., B.A.Y.: collection and/or assembly of data and data analysis and interpretation; C.J.R., S.N.U., and A.J.L.: collection and/or assembly of data; P.J.C.: data analysis and interpretation, manuscript writing, and final approval of manuscript; S.C.: conception and design of the study, financial support, data analysis and interpretation, manuscript writing, and final approval of manuscript.

Disclosure of Potential Conflicts of Interest

The authors indicate no potential conflicts of interest.

References

1 Ogawa M, Larue AC, Mehrotra M. Hematopoietic stem cells are pluripotent and not just "hematopoietic". Blood Cells Mol Dis 2013;51:3–8.

2 Wang X, Willenbring H, Akkari Y et al. Cell fusion is the principal source of bone-marrow-derived hepatocytes. Nature 2003; 422:897–901.

3 Ratajczak MZ, Kucia M, Jadczyk T et al. Pivotal role of paracrine effects in stem cell therapies in regenerative medicine: Can we translate stem cell-secreted paracrine factors and microvesicles into better therapeutic strategies? Leukemia 2012;26:1166–1173.

4 Cherqui S, Sevin C, Hamard G et al. Intralysosomal cystine accumulation in mice lacking cystinosin, the protein defective in cystinosis. Mol Cell Biol 2002;22:7622–7632.

5 Nevo N, Chol M, Bailleux A et al. Renal phenotype of the cystinosis mouse model is dependent upon genetic background. Nephrol Dial Transplant 2010;25:1059–1066.

6 Nesterova G, Gahl W. Nephropathic cystinosis: Late complications of a multisystemic disease. Pediatr Nephrol 2008;23:863–878.

7 Kalatzis V, Cherqui S, Antignac C et al. Cystinosin, the protein defective in cystinosis, is a H(+)-driven lysosomal cystine transporter. EMBO J 2001;20:5940–5949.

8 Harrison F, Yeagy BA, Rocca CJ et al. Hematopoietic stem cell gene therapy for the multisystemic lysosomal storage disorder cystinosis. Mol Ther 2013;21:433–444.

9 Syres K, Harrison F, Tadlock M et al. Successful treatment of the murine model of cystinosis using bone marrow cell transplantation. Blood 2009;114:2542–2552.

10 Yeagy BA, Harrison F, Gubler MC et al. Kidney preservation by bone marrow cell transplantation in hereditary nephropathy. Kidney Int 2011;79:1198–1206.

11 Beck M. Therapy for lysosomal storage disorders. IUBMB Life 2010;62:33–40.

12 Rustom A, Saffrich R, Markovic I et al. Nanotubular highways for intercellular

organelle transport. Science 2004;303:1007–1010.
13 Chinnery HR, Pearlman E, McMenamin PG. Cutting edge: Membrane nanotubes in vivo: A feature of MHC class II+ cells in the mouse cornea. J Immunol 2008;180:5779–5783.
14 Islam MN, Das SR, Emin MT et al. Mitochondrial transfer from bone-marrow-derived stromal cells to pulmonary alveoli protects against acute lung injury. Nat Med 2012;18:759–765.
15 Onfelt B, Nedvetzki S, Benninger RK et al. Structurally distinct membrane nanotubes between human macrophages support long-distance vesicular traffic or surfing of bacteria. J Immunol 2006;177:8476–8483.
16 Marzo L, Gousset K, Zurzolo C. Multifaceted roles of tunneling nanotubes in intercellular communication. Front Physiol 2012;3:72.
17 Sowinski S, Alakoskela JM, Jolly C et al. Optimized methods for imaging membrane nanotubes between T cells and trafficking of HIV-1. Methods 2011;53:27–33.
18 Rogers RS, Bhattacharya J. When cells become organelle donors. Physiology 2013;28:414–422.
19 Wang X, Gerdes HH. Long-distance electrical coupling via tunneling nanotubes. Biochim Biophys Acta 2012;1818:2082–2086.
20 Hohenester E, Yurchenco PD. Laminins in basement membrane assembly. Cell Adh Migr 2013;7:56–63.
21 Abrahamson DR, Leardkamolkarn V. Development of kidney tubular basement membranes. Kidney Int 1991;39:382–393.
22 Halfter W, Candiello J, Hu H et al. Protein composition and biomechanical properties of in vivo-derived basement membranes. Cell Adh Migr 2013;7:64–71.
23 Linder S, Wiesner C, Himmel M. Degrading devices: Invadosomes in proteolytic cell invasion. Annu Rev Cell Dev Biol 2011;27:185–211.
24 Hagedorn EJ, Kelley LC, Naegeli KM et al. ADF/cofilin promotes invadopodial membrane recycling during cell invasion in vivo. J Cell Biol 2014;204:1209–1218.
25 Hagedorn EJ, Ziel JW, Morrissey MA et al. The netrin receptor DCC focuses invadopodia-driven basement membrane transmigration in vivo. J Cell Biol 2013;201:903–913.
26 Yu X, Zech T, McDonald L et al. N-WASP coordinates the delivery and F-actin-mediated capture of MT1-MMP at invasive pseudopods. J Cell Biol 2012;199:527–544.
27 Burgess AW, Metcalf D, Kozka IJ et al. Purification of two forms of colony-stimulating factor from mouse L-cell-conditioned medium. J Biol Chem 1985;260:16004–16011.
28 Weischenfeldt J, Porse B. Bone marrow-derived macrophages (BMM): Isolation and applications. CSH Protoc 2008;2008:pdb prot5080.
29 Dull T, Zufferey R, Kelly M et al. A third-generation lentivirus vector with a conditional packaging system. J Virol 1998;72:8463–8471.
30 Zychlinski D, Schambach A, Modlich U et al. Physiological promoters reduce the genotoxic risk of integrating gene vectors. Mol Ther 2008;16:718–725.
31 Camussi G, Deregibus MC, Bruno S et al. Exosomes/microvesicles as a mechanism of cell-to-cell communication. Kidney Int 2010;78:838–848.
32 Iglesias DM, El-Kares R, Taranta A et al. Stem cell microvesicles transfer cystinosin to human cystinotic cells and reduce cystine accumulation in vitro. PLoS One 2012;7:e42840.
33 Thoene J, Goss T, Witcher M et al. In vitro correction of disorders of lysosomal transport by microvesicles derived from baculovirus-infected Spodoptera cells. Mol Genet Metab 2013;109:77–85.
34 Zomer A, Vendrig T, Hopmans ES et al. Exosomes: Fit to deliver small RNA. Commun Integr Biol 2010;3:447–450.
35 Wang Y, Cui J, Sun X et al. Tunneling-nanotube development in astrocytes depends on p53 activation. Cell Death Differ 2011;18:732–742.
36 Yasuda K, Khandare A, Burianovskyy L et al. Tunneling nanotubes mediate rescue of prematurely senescent endothelial cells by endothelial progenitors: Exchange of lysosomal pool. Aging 2011;3:597–608.
37 Luzio JP, Pryor PR, Bright NA. Lysosomes: Fusion and function. Nat Rev Mol Cell Biol 2007;8:622–632.
38 Cherqui S, Kalatzis V, Trugnan G et al. The targeting of cystinosin to the lysosomal membrane requires a tyrosine-based signal and a novel sorting motif. J Biol Chem 2001;276:13314–13321.
39 Humphreys BD. Kidney injury, stem cells and regeneration. Curr Opin Nephrol Hypertens 2014;23:25–31.
40 Yeagy BA, Cherqui S. Kidney repair and stem cells: A complex and controversial process. Pediatr Nephrol 2011;26:1427–1434.
41 Chevronnay HP, Janssens V, Van Der Smissen P et al. Time-course of pathogenic and adaptive mechanisms in cystinotic mice kidneys. J Am Soc Nephrol 2014;25:1256–1269.


See www.StemCells.com for supporting information available online.